University of Bath

Alternative formats
If you require this document in an alternative format, please contact:
openaccess@bath.ac.uk

Decyltrimethylammonium bromide micelles in acidic solutions: counterion binding, water structuring and micelle shape

Daniel T. Bowron[a] and Karen J Edler[b*]

a. ISIS, Science and Technology Facilities Council Rutherford Appleton Laboratory, Harwell Oxford, Didcot OX11 0QX, UK

b. Department of Chemistry, University of Bath, Claverton Down, Bath, BA2 7AY, UK

* author for correspondence, k.edler@bath.ac.uk.

Abstract

Wide-angle neutron scattering experiments combined with Empirical Potential Structural Refinement modelling have been used to study the detailed structure of decyltrimethylammonium bromide micelles in the presence of acid solutions of HCl or HBr. These experiments demonstrate considerable variation in micelle structure and water structuring between micelles in the two acid solutions and in comparison with the same micelles in pure water. In the presence of the acids, the micelles are smaller, however in the presence of HCl the micelles are more loosely structured and disordered while in the presence of HBr the micelles are more compact and closer to spherical. Bromide ions bind strongly to the micelle surface in the HBr solution, while in HCl solutions, ion binding to the micelle is similar to that found in pure water. The hydration numbers of the anions and extent of counterion binding follow the predictions of the Hofmeister series for these species.

Introduction

Cationic surfactants have myriad uses in many industries, including wetting, foaming, emulsification, rheology modification and as dispersing agents.[1] They are frequently applied in detergents and

1

dispersants in applications from personal care to pharmaceutics. Cationic quaternary ammonium surfactants are also commonly used as templates in syntheses of mesoporous silica. In these preparations, the pH is either alkaline, producing a powder usually with little defined macroscopic structure, or acidic, where formation of well-defined "single crystals", twisted gyroid shapes,[2-3] uniform spheres[4] or thin films[5] occurs. In the acidic syntheses, the polymerising silica carries a transient positive charge arising from a 5-coordinate intermediate,[6] so the mechanism by which the positively charged silica interacts with the positively charged micelle has been suggested to involve a mediating counteranion.[7] Synthesis of mesoporous silicas via the acidic route using cetyltriethylammonium bromide surfactant with a range of different acids also produced changes the mesostructure of the final silica materials.[8] The change in curvature of the micelles was ascribed to the binding of the anion from the acid, resulting in headgroup area changes. This led to changes in the micelle shape, as well as in its interactions with the silica, related to the decreasing charge density as polymerisation continued, which led to phase changes during synthesis. The anion present also affects the long range ordering of mesophases in alkaline surfactant templated silica syntheses where the surfactant and silica have opposite charges. Greater long range order has been reported when H_2SO_4 was added to a synthesis at pH 10, compared to that seen for HCl.[9] Work using addition of sodium halide salts to the synthesis of mesoporous silicas templated using a range of alkyltrimethylammonium bromide templates from C_{10}-C_{16} in alkaline solutions, has also shown variation in the rate of reaction, and formation of ordered mesostructures which was ascribed to differences in counterion binding to the micelle surface.[10] Anion interactions with the micelle surface therefore are important to mediate the interaction of cationic surfactant templates with the polymerising silica, in both acidic and alkaline solutions. The details of ion binding in these solutions, with multiple competing counterions, are yet to be resolved, but may provide insights into structuring observed, not only on the nanoscale, but also on larger scales in these systems.

Ion binding and competition at interfaces has long been of interest in many fields utilizing amphiphile self assembly, including biphasic reactions and catalysis.[11] Techniques such as EPR,[12] ion specific electrodes[13], chemical trapping[14-15] and spectroscopic methods[16-20] have been used to measure ion binding and hydration at micelle surfaces. Most of these techniques give averaged information from the solutions and it can be difficult to define the precise location of "bound" vs "free" counterions,[21] however they have been extensively used to determine a general picture of ion binding to micelles.

More recently there has been renewed interest in the extent and specificity of ion binding to charged interfaces in solution for more general cases of soft interfaces as well as those present in micellar solutions,[22-23] such as liquid crystalline phases,[24] lipid membranes[19, 25] and at the protein-water interface.[26] Ion binding is known to depend not only on the charge but also the ion radius and polarizability, among other factors, empirically incorporated in the Hofmeister series.[27-28] The Hofmeister series ordering, originally based on the ability of ions to precipitate or promote dissolution of proteins in aqueous solutions, has been the focus of many recent reports probing the underlying interactions responsible for ion binding to such interfaces.[27, 29-31] A variety of techniques including Langmuir isotherms,[32] spectroscopic techniques,[18-20] X-ray reflectivity and fluorescence,[33] rheology,[22] small angle scattering,[24] as well as modelling and simulation studies[19, 34] have been directed at determining the extent and types of adsorption of ions to such interfaces.

In this paper we have begun a study of the effects of addition of counteranions to positively charged decyltrimethylammonium bromide ($C_{10}TAB$) micelles, as a precursor to studies of these micelles in the presence of silica and to understand the effect of mixed anions compared to co-ions on micelle size, shape and surfactant ordering, since ion mixtures are more commonly used in such syntheses. Specifically we wished to understand the nature of counteranion binding to the surface of the micelles, and the effects of acid addition upon micelle structure. $C_{10}TAB$ is a model quaternary ammonium surfactant in the same class as $C_{16}TAB$, typically used in the synthesis of mesoporous silicas. $C_{10}TAB$

has a shorter hydrocarbon chain, thus a smaller micelle size, making it more amenable to the data modelling approach chosen in this work. We chose HCl, as the acid typically used in mesoporous silica synthesis, and HBr to contrast the behaviour of adding extra anions of the same type as those present in the surfactant, with those where the added anions are different. The acid concentration, 0.2 M was chosen to match that used in the synthesis of interfacial surfactant-templated silica films.[5, 35]

The effect of added counterions on the size and shape of decyltrimethylammonium surfactant micelles has been studied extensively, for many years, using small angle scattering techniques and light scattering which have a relatively low resolution. These studies include an early study by Debye (1949) which concluded that for $C_{10}TAB$, little change in micelle size and shape was observed upon addition of 0.013 M KBr, although larger changes were observed for surfactants with a longer hydrophobic tail.[36] This is corroborated by a number of more recent studies.[37]

The binding of counterions to micelles formed from decyltrimethylammonium bromide has also been extensively studied for single counterion cases. For $C_{10}TAB$ in water, a range of values is found for the fraction of dissociated bromide counterions, β, varying from 0.22- 0.42.[13, 37-38] However in general it is found that β is constant over large variation of conditions of micelle concentration, added salt and temperature,[39] thus the interfacial concentration of counterions increases with increasing surfactant concentration in solution.[40] Counterion binding to micelle surfaces is also dependent on micelle size, with smaller micelles showing little change in fractional charge as salt concentrations are increased (up to 100 mM).[41] However counterion condensation onto the micelle does depend on the counterion used; the counterion binding to the micelle decreases as the hydrated size of the counterion increases.[42]

In binary ion containing systems, competitive ion binding at the micelle surface has been studied using techniques including chemical trapping, for C_nTA^+ surfactants with n=12-16. These experiments reveal a stronger binding of Br^- than Cl^- to the surface of C_nTA^+ micelles when both species are present.[14, 43-]

[44] Interestingly the selectivity towards binding of Cl⁻ becomes slightly stronger as the mole fraction of Br⁻ is increased, despite the large increase in the fraction of surface covered by Br⁻ at high Br⁻ mole fraction.[14] Thus in mixed systems the effects of ion binding are not always additive.[44] These studies supply information on the relative concentrations of ions in the headgroup region but cannot access the locations of ion binding around the headgroup and their relationship to water binding sites. In this work therefore in addition to the effects on micelle shape and size, we aimed to discover the location of the added counterions and their effect on the water structure at the headgroups of the surfactants within the micelle, since these parameters will alter potential binding sites for silica species during synthesis of mesoporous materials.

Experimental Section

Decyltrimethylammonium bromide (hC_{10}TAB, purity 99 %) from Acros Organics and D_2O (99.9 atom%D), HCl and HBr were obtained from Sigma Aldrich. All were used without further purification. Fully deuterated d30-C_{10}TAB and tail-deuterated d21-C_{10}TAB were obtained from the Oxford Isotope Laboratory and were also used without further purification. Ultrapure water with 18.2MΩ cm resistance was also used to prepare solutions for measurement. Solutions of C_{10}TAB in 0.2 M HCl or 0.2 M HBr (1.5 ml for solutions containing d-surfactants, 2 ml for h-surfactant solutions) were prepared at 0.4 M C_{10}TAB by weighing the required amount of surfactant into a vial, adding the required weight of 0.2 M acid solution in H_2O or D_2O and shaking briefly until dissolved. The following set of samples was prepared for 0.2 M HCl solutions: hC_{10}TAB in D_2O, d30-C_{10}TAB in D_2O, d30-C_{10}TAB in H_2O, d30-C_{10}TAB in 50 mol% D_2O/50 mol% H_2O (referred to as HDO), 50 mol% hC_{10}TAB/ 50 mol% d30-C_{10}TAB in D_2O, d21-C_{10}TAB in D_2O. However for the 0.2 M HBr solutions, limitations on available beamtime meant that only 3 samples were measured: d30-C_{10}TAB in D_2O, d30-C_{10}TAB in H_2O, d30-C_{10}TAB in HDO. Using parameters from the 0.2 M HCl samples, these three contrasts were however sufficient to probe differences between C_{10}TAB micelles in HCl versus HBr solutions.

Samples were measured on the SANDALS time-of-flight diffractometer on Target Station 1 at ISIS Spallation Neutron Source in Oxfordshire. SANDALS is designed for measurement of samples containing light elements and covers a Q range of 0.1 to 50 Å^{-1}. The C_{10}TAB solutions were loaded into 1 mm wide null-scattering flat plate TiZr cells with a 1mm wall thickness, and a beam with a circular diameter of 30 mm was used for the measurements. Cells were sealed using a Teflon o-ring, and tested against vacuum at 25 °C before loading into the sample changer on the instrument. Each sample was measured for 500 μA proton beam current (roughly 8 hours). Empty cell backgrounds and a 3 mm thick vanadium plate calibration standard were measured for an equivalent amount of time.

Empirical Potential Structure Refinement

Since our preliminary investigation[45] of the atomistic structure of surfactant micelles formed in 0.4 M C_{10}TAB aqueous solutions at 25 °C, improvements in the core Empirical Potential Structure Refinement (EPSR) methodology[46] through the implementation of parallel processing methods for the more computationally intensive aspects of the computer algorithms, have now made it practical to investigate such complex systems on a far more routine basis. Current performance of EPSR, based on using a personal workstation running a 12 core Intel Xeon X5690 CPU at 3.47GHz, typically allows us to refine atomistic models of systems containing 100000 atoms in approximately two weeks. This step change in performance corresponds in practicality to an increase in system size of a factor four in the number of atoms in the model and a speed increase in which the larger model is delivered approximately ten times faster than the original containing 26304 atoms.

Based on these new atomistic data refinement capabilities we have investigated three models of 0.4 M C_{10}TAB surfactants. Two models incorporating the additional component of 0.2 M acid, and a third model on the acid free solution to ensure that all comparisons between derived structural parameters are consistent and as free from system size effects as possible. This third acid-free model is essentially a repeat of our earlier study[45] in which the model size has been increased to consist of 256 $C_{10}TA^+$

cations, 256 Br$^-$ anions and 31232 water molecules in a cubic box of side length 101.71 Å. The 0.4 M

C$_{10}$TAB in 0.2 M HCl model was then constructed as a model containing 256 C$_{10}$TA$^+$ cations, 256 Br$^-$

anions with 124 H$^+$ cations, 124 Cl$^-$ anion and 31232 water molecules, in a cubic box of side 101.79 Å.

Correspondingly the 0.4 M C$_{10}$TAB in 0.2 M HBr model was built with 256 C$_{10}$TA$^+$ cations, 380 Br$^-$

anions with 124 H$^+$ cations and 31232 water molecules in in a simulation box of identical size. In all

cases the simulation box was sized to match an atomic density for the solution of 0.1 atoms Å^{-3}. The

atoms in each molecule are referred to by abbreviated forms as labelled in Figure 1. The Lennard-Jones

and Coulomb charge parameters used for the reference potentials that are required to seed the models,

are given in Supporting Information, Table S1, and within each model, the structure of the molecules
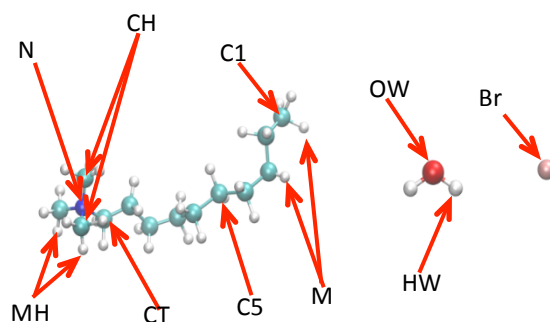
were defined as previously reported.[45]

Figure 1: Nomenclature of atoms in C$_{10}$TAB and water used in the EPSR analysis. Not shown are the

hydrogen and chloride ions that were incorporated in similar fashion to the bromide ions.

As in our original study, the starting configurations of the models consisted of a uniform distribution of

un-associated surfactants, ions and water molecules that had been allowed to equilibrate under the

reference potential scheme. Tests confirmed that no micelles were formed within the models until the

structural information from the neutron scattering data was incorporated into the structure refinement

process via the development of the empirical perturbation potential calculated out to an atomic pairwise

interaction distance of 25 Å. The EPSR simulation was first run for a number of Monte-Carlo cycles,

which attempt to move every atom, each freely rotating group and to translate every molecule in the

box, in order to equilibrate in energy. After equilibration the empirical potential was introduced to refine the model against the experimental neutron data, and 5000 refinement cycles were run, generating 15000 configurations. In this work statistical data was collected during this period after each five Monte-Carlo refinement cycles, to obtain the radial distribution functions, spatial density functions and intermolecular coordination numbers, which are therefore averaged over 3000 configurations. Following the methodology of our earlier study,[45] surfactant monomers were considered to be "bound" in an aggregate if any of the last four carbon atoms in the surfactant tail (C1-C4) were found to be within 5 Å of any of the equivalent carbon atoms on a neighbouring surfactant molecule.
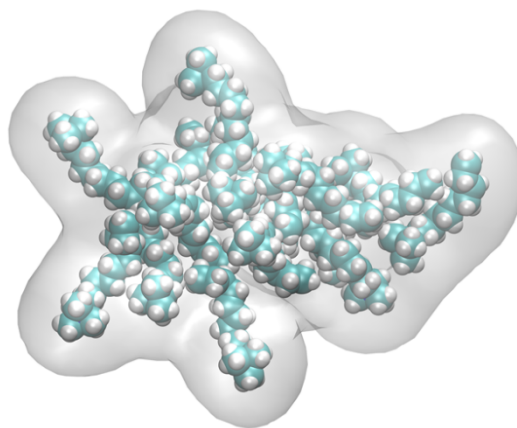

Figure 2: Illustration of an example test surface, which wraps an aggregated molecule structure at a distance of 1Å from the outermost atoms. The surface is shown in grey around the surfactant molecules which make up a micellar aggregate displaying levels of structural disorder that preclude the use of simple bounding surface calculations based on idealized micelle structural geometries. (Colour scheme as in Figure 3).

As one of the primary aims of this study was to investigate the effect of acid on the morphology of the micelles and the anion distribution around the positively charged micelle surface, it was necessary to

develop a robust means to calculate the properties associated with outer surface of the micelles generated in the molecular configurations generated during final ensemble averaging stage of the EPSR procedure. To this end, for each micelle investigated in the model, a test surface (Figure 2) that wraps the micelle structure at a distance of 1 Å from the outermost atoms was constructed via a Monte Carlo method. In this approach the algorithm calculates many thousands of test points within a volume encompassing the micelle, and this process continues to run until a specified number of points e.g. 10000, are found that meet the distance criterion from the outermost atoms and thus define the surface. Having generated a wrapping surface, it is then a trivial matter to calculate parameters such as the number of cations (N_{cation}) that are found within 2.5 Å of the inner side of this surface, and the number of anions (Br$^-$ and Cl$^-$) that are found within ±1.5 Å of this surface. Once the number of cations and anions at the surface of the micelle is known, the β parameter, defined as 1.0-($<N_{anion}>/<N_{cation}>$), can be determined.

Results

Neutron scattering combined with EPSR provides an atomistic picture of the species in this system. At a concentration of 0.4 M $C_{10}TAB$, the solutions are well above the expected CMC for this surfactant, which is around 0.06 M at 25 °C.[47-49] Snapshots of the configuration of molecules in the EPSR simulation taken after the total energy of the system has equilibrated, clearly show the aggregation of the $C_{10}TAB$ molecules into clusters in the solutions studied (Figure 3). Averaging of all equilibrated snapshots over 3000 configurations produces the fits to the data sets shown in Figure 4 and Supporting information, Figures S1 and S2. The fitted line averaged from all configurations generated at equilibrium was checked by assessing how close it matched both Q-space and real space data (see residuals Figure 4). The fit residuals demonstrate that the EPSR refined model captures the low-Q data features that are indicative of the presence of aggregated micelle structures in the models (see fits and residuals shown in Figure 4 and Supporting information, Figure S1). The real space functions, F(r), the

Fourier transform of F(Q), gave correct values for intramolecular structure (ie bond distances within molecules) and first neighbour inter-molecular structure (e.g. water-water distances are very close, if not identical to those for bulk water). Figure S2, supporting information shows that the models also capture the short-range atomic pair correlations in the solution. Figures S3 and S4, supporting information, show similar fits for acid free solutions of 0.4 M $C_{10}TAB$, for comparison. A slight discrepancy between the model fit and experimental data at the lowest Q values (highlighted in the low Q expansion, Figure 4, right) for C10TAB-D in HDO, may be due to a small weighing error during sample preparation, leading to a slight error in the isotopic composition of this sample.
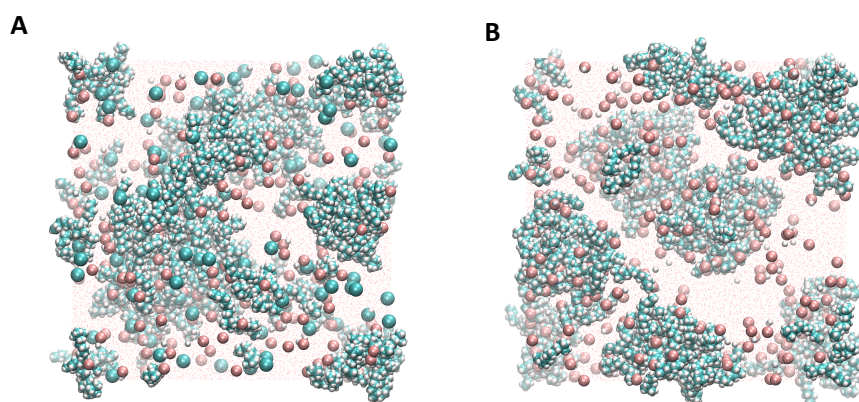

Figure 3: Snapshots after micelle formation of a 256 $C_{10}TAB$ EPSR (0.4 M $C_{10}TAB$) simulation for data taken in the presence of 0.2 M acid at 25°C (A) HCl (B) HBr. Colour scheme: medium sized pink spheres are the bromide ions (A & B), large green spheres are chloride ions (A), medium sized teal spheres are the carbon atoms in $C_{10}TAB$ molecules, the medium blue spheres are the nitrogen atom in the headgroup of the $C_{10}TAB$ molecule (which are mostly masked by the spheres of the carbon atoms), and the small red dots in the background are the oxygen atoms belonging to the water molecules which have been minimised in size to allow the surfactant aggregates to be more easily seen.
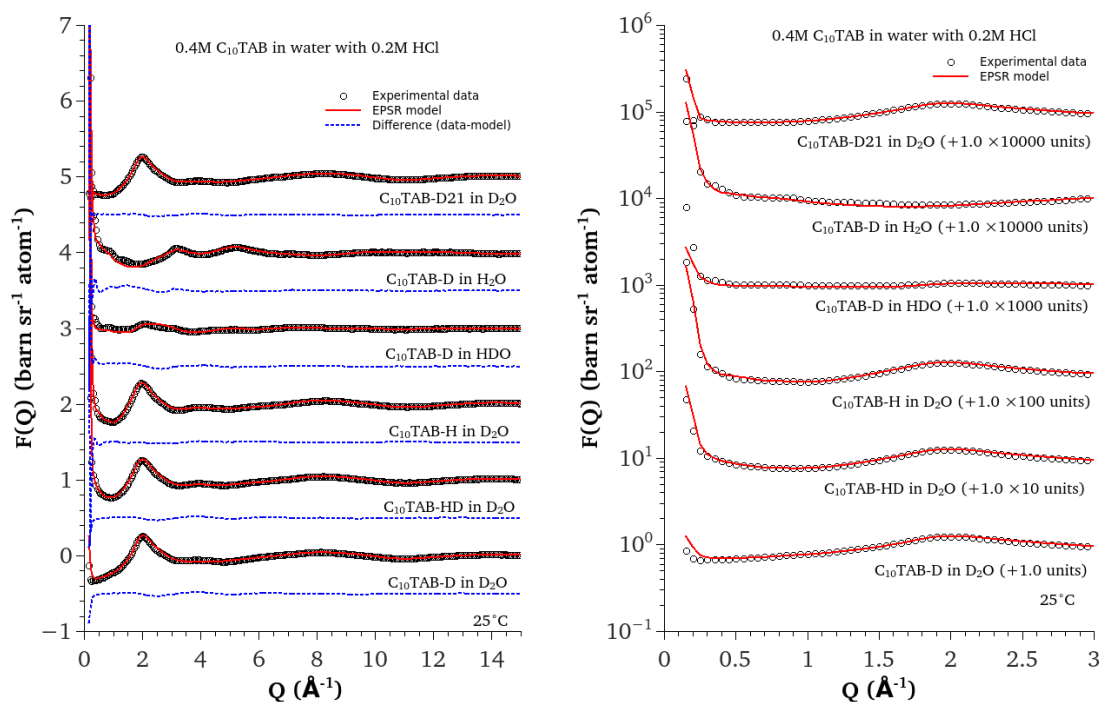
Figure 4. EPSR model fit for 0.4 M C$_{10}$TAB in 0.2 M HCl (solid red lines) and fit residuals (dashed blue lines offset by 1.0 down the ordinate axis) to the diffraction data (black circles) of the five isotopic samples. A single model was used to fit all of the available data sets, which have different neutron contrast. The right hand graph expands the low Q region to highlight the fits to the data in this region. For clarity, each data set is offset up the ordinate, and each residual offset from its data set. The corresponding figures for the 0.2 M HBr system and the acid free models can be found in supporting information, Figures S1 and S3.

Discussion

From the models determined above, we can extract information on the average micelle sizes, the atomic density distributions within the micelles, and details of the arrangement of counterions and water around the surfactant headgroups in the vicinity of the micelles.

The first striking result of such analysis is that the addition of both acids leads to more well-defined micellar aggregates, with greater uniformity and smaller size compared to micelles of the same

surfactant in pure water (Figure 5, Table 1). The information in Figure 5 shows the probability distribution of aggregates in the models as a function of the number of $C_{10}TA$ units. From this, it can be seen that 73.4% (pure water), 79.5% (HBr) and 69.1% (HCl) "aggregates" contain only 1 $C_{10}TA$ unit. In addition in all systems there are significant numbers of dimers, trimmers and tetramers in the system in addition to the larger micellar aggregates. In comparison with the total number of aggregates present, the probability of micelle-sized aggregates is therefore small (Figure 5) although they are obviously present in the models when inspected by eye. Thus here, particularly in the acid solutions, for concentrations considerably above the CMC, the typical description of a micellar solution as containing residual monomers and micelles rather than a range of aggregates sizes is not a particularly realistic approximation. However in pure water, the micelle size does show distinct peaks indicating favoured aggregation numbers, while in the solutions with added acids, the distributions are almost continuous.
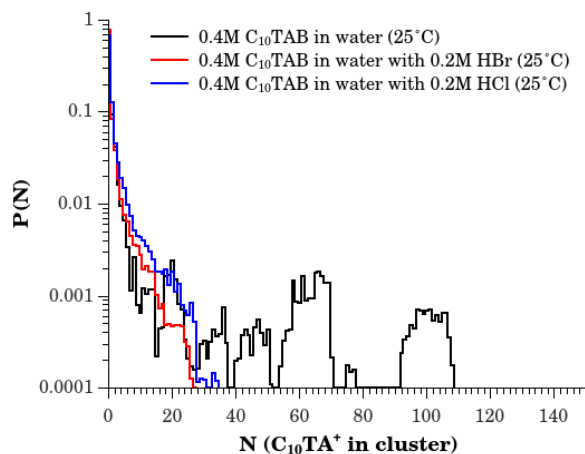
Figure 5: Comparison of micelle cluster sizes in $C_{10}TAB$ micelles in the presence and absence of 0.2 M acid. P(N) is the number of clusters of size N divided by the total number of clusters in the box.

In the pure water system, for the data analysed here, the micelle sizes extend to much larger aggregates, and appear to form in discrete size ranges that are most likely caused by the aggregation of smaller micellar structures of favoured sizes as they move around the simulated volume of the system. Given that all three simulations were performed in similar size simulation boxes, and that no aggregates form

using only the reference parameters, until the feedback via the use of the empirical potential derived from the neutron scattering data is turned on, we do not believe this is an artefact of the simulation. Therefore, these distributions must arise from the information available in the neutron scattering data. In EPSR, there is possibly a bias to retaining larger entities for longer than they may exist in reality, as the driving force to pull them apart is not manifest strongly in the data. However , the size of the largest micelles in each simulation box appears to be stable once formed, and we have checked in our previous work that box size does not affect the average size of the largest aggregate formed.[45] We note that the radius of gyration for the largest micelles in this simulation (averaged over 3000 configurations) is 22.1±3.8 Å, which is, within error, similar to the value of micelle radius for $C_{10}TAB$ in water, found by NMR,[50] of 17.7 Å. Therefore our discussion of the results will now concentrate on the largest aggregate formed in each simulation box to determine the properties of the micelles in these simulations.
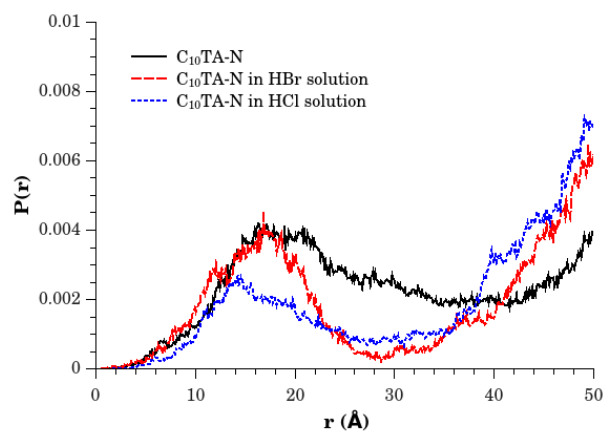
Figure 6: Direct comparison between the atomic density profiles, measured from the centre of mass and averaged over the largest micellar aggregate found in each configurational ensemble generated in the structural modeling process, for the decyltrimethylammonium nitrogen sites ($C_{10}TA-N$) in 0.4 M $C_{10}TAB$ solutions, without acid and with 0.2 M HCl and HBr.

The effect of cluster size with and without acid can also be seen in the atomic density profiles in Figure

6, where the position of the nitrogen in the surfactant headgroup is plotted relative to the centre of the micelles. The nitrogen distribution for the pure water case is at a maximum over a range of 16-20 Å from the micelle centre while for the micelles in 0.2 M HCl and HBr the nitrogen distribution is in both cases more strongly peaked, and closer to the micelle centre. Additionally, comparing the case for the $C_{10}TAB$ micelles with added HBr to that with added HCl, the extra Br⁻ ions lead to a tighter packing of molecules in the micelles than when HCl is added (resulting in an aggregate which is closer to spherical) and thus a more well-defined micelle "surface". In the atomic density profiles presented in Figures 6 and 7, although the micelles in the two solutions are similar in size, the nitrogen distribution relative to the centre of the micelle is more strongly peaked around 17 Å from the micelle centre for the solution containing HBr. For the solution containing HCl, the distribution is peaked closer to the micelle centre, at around 14 Å but the peak is lower and extends over a broader range of distribution of $C_{10}TA$-N sites.

Comparing the penetration of water into the micelles with and without added acids, the atomic density profiles of several components, shown in Figure 7, suggests that for micelles in the HBr solution, the central 12 Å remains dry, while in pure water or with 0.2 M HCl, water penetrates up to 2 Å further towards the micelle centre. In the HBr solution and in pure water, the water distribution also rises more sharply after the peak of the N distribution, while it has an intermediate slope in the presence of the HCl. Earlier SANS experiments on tetradecyltrimethylammonium bromide[51] and hexadecyltrimethylammonium[14, 43] ($C_{16}TAB$) micelles has suggested that upon addition of NaBr the micelles become dehydrated, since the addition of NaBr leads to a reduction of the chemical potential of the water. This appears to corroborate our results, since the micelles in the presence of NaBr contain less water near the headgroups than in the other two systems. It can also be seen in Figure 7 that the position of the first carbon on the alkyl chain (ie the carbon furthest from the surfactant headgroup) is also more well defined in the case of the micelles in the HBr solution while the position of this moiety

is smeared out in the case of the more disordered HCl solution micelle. Micelles are of course dynamic structures, so this smearing out of the carbon position may indicate that exchange of surfactant cations between micelles occurs more frequently in the HCl solution, leading to the observed wider range of locations for the tail carbons.
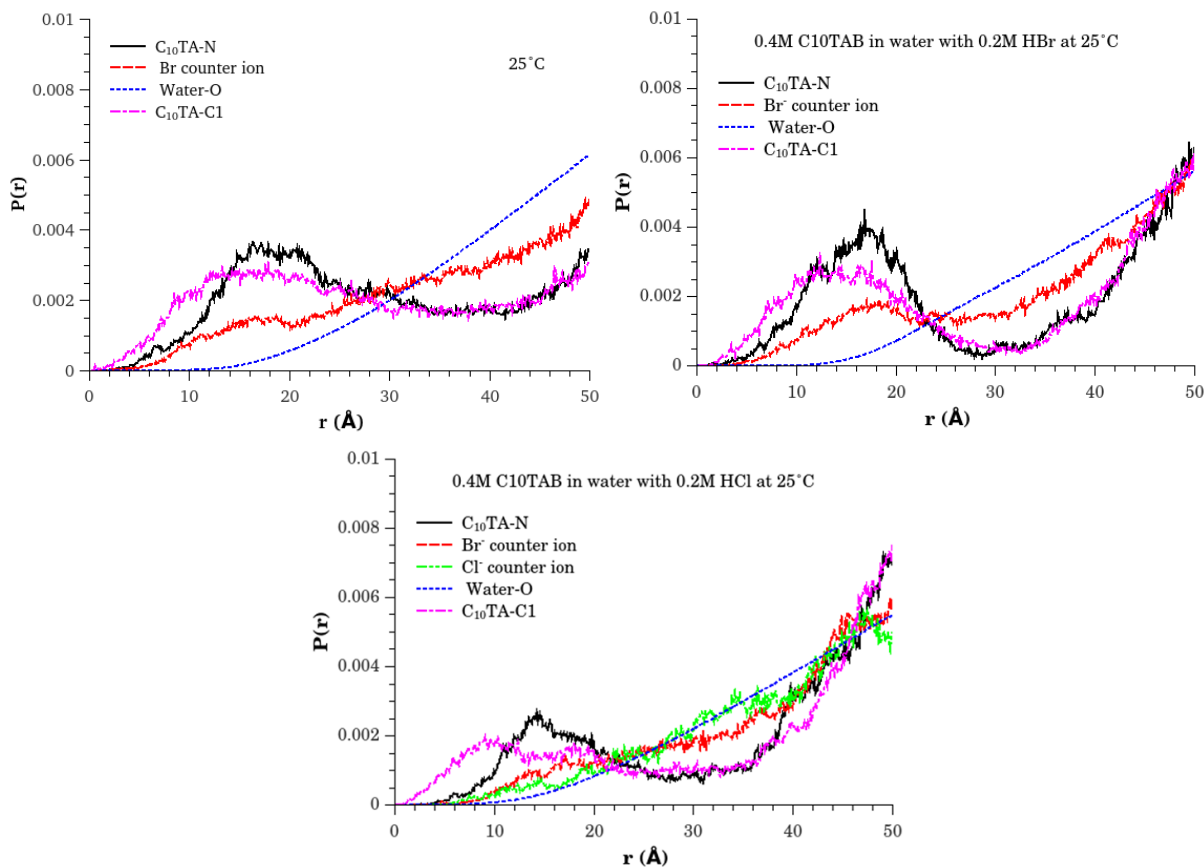
Figure 7: Comparison of atomic density profiles calculated from the centre of the largest micelle in the model box, for the 0.4 M C_{10}TAB solutions in (top left) water (top right) 0.2 M HBr and (right) 0.2 M HCl. The functions relate to illustrative atomic sites; the decyltrimethylammonium nitrogen sites (C_{10}TA-N), the bromide counter ion sites (Br), the water oxygen sites (Water-O) and the carbon in the surfactant tail that is furthest from the polar trimethylammonium head group (C1).

When considering the anion distribution we note that the neutron data is not very sensitive to the identity of the ions due to their low overall concentration in these solutions, meaning there are no strong markers in the data that distinguish between them. However the identities and location of these low-weighted structural components are reflected in the model through the reference potential, which defines the size of those ions, and the Coulomb charge that dominates how they interact with other charged atomic sites. Thus we observe distinct binding differences for Cl⁻ and Br⁻ in our model which enable comparison with counterion binding determinations using other techniques. In the C_{10}TAB solution with 0.2 M HBr, the bromide is more tightly associated with the nitrogen in the surfactant headgroups than the mixed chloride/bromide anions are in the HCl case (Figure 7). This provides evidence for a higher degree of anion binding to the micelle surface in the case where only Br⁻ anions are present, as predicted by the Hofmeister series,[27] which ranks anions in order of their ability to "salt out" (ie precipitate) proteins, polymers or micelles in solution. The cause of the Hofmeister series is still a matter of debate[28, 31] but it appears to involve the hydration strength of the ion (the extent to which water binds to that ion) and its hydrophobicity. Van der Waals interactions between the species are also important, giving rise to attractive interactions between solution components.[52] Chloride ions are known to associate much less strongly with micelle surfaces than bromide ions, and are more strongly hydrated. In the distributions in Figure 7, for the micelles in 0.2 M HCl solution the total number of both anions near the nitrogen headgroups are lower than numbers of the Br⁻ at this radius for micelles in pure water or HBr solution. In the HCl solution the Cl⁻ distribution exceeds that of the Br⁻ at large distances from the micelle surface, in the bulk water part of the model. In systems containing only one ion type, chloride typically is described as being around 20-30% bound to a cationic micelle surface, compared to 70% for bromide.[51] However, less work has been reported on total bound ion concentration in mixtures of Hofmeister series ions. Loughlin and Romsted[14] note that the total concentration of interfacial counterions on C_{16}TAX micelles increases as the overall concentration of halide ions, X in solution is increased, which is also observed for both acids added here. Although the

effects of Cl⁻ and Br⁻ have been noted to be additive when small amounts of NaBr are added to a solution containing 0.1M NaCl, more complex effects are observed for the reverse case, where, similar to our case here, small amounts of NaCl were added to a solution of constant 0.1M NaBr. This was ascribed to competition between these counterions for hydration water as the added Cl⁻ perturbs the initial water structure around the Br⁻ ions.[44] This may account for drop in the total number of anions per surfactant molecule in the micelle between cases with added 0.2 M HCl (total anions/N_{agg} = 0.48) compared to 0.2 M HBr (total anions/N_{agg} = 0.79) observed in Table 1. In both cases the total number of anions per surfactant molecule in the micelle is higher in the presence of the acids than for pure water (total anions/N_{agg} = 0.39), as expected, since the total anion concentration in solution is higher.

The equilibrium constant for anion exchange at the micelle surface, $K = \frac{[Br_m][Cl_w]}{[Cl_m][Br_w]}$, (where X_m is the ion concentration bound to the micelle, and X_w is the ion concentration in solution) can be calculated for the ion distribution in the simulation box for the $C_{10}TAB$ in 0.2 M HCl data to be around 1.4. This contrasts with earlier work on competitive counterion binding to micelle surfaces using chemical trapping techniques where it is suggested that a 1:1 mixture of Br⁻ and Cl⁻ in the bulk solution at low surfactant concentration (0.01 M) results in K = 3-5.[14] Loughlin and Romsted did however demonstrate that, in solutions containing hexadecytrimethylammonium halide micelles plus salt, as the mole fraction of Br⁻ was increased, a small but significant increase in selectivity toward Cl⁻ by the micelle surface was observed despite the large increase in the fraction of surface covered by Br⁻ at high Br⁻ mole fraction.[14] Thus our neutron diffraction data shows a similar trend to these chemical trapping experiments but to a lesser degree, since the mole fraction of Br⁻ in our solutions is higher than that of Cl⁻. Values of K, also called the selectivity ratio for ion binding, determined for other ratios of Br:Cl, for a wide range of amphiphiles, using a number of different techniques range from 1.7 to 6.[16, 53-56] We note that our calculation of K ignores any counterions bound to smaller aggregates in the box, since our analysis uses only the largest micelle present in each box to derive the numbers in Table 1, and also

that in our case $[Cl_{total}]/[Br_{total}] = 0.5$ and the total halide ion concentration is only 0.6 M – both of these factors were shown to reduce K in Loughin & Romsted,[14] so our results are not out of line with earlier work.

Table 1: Average properties of the largest micelle in each simulation box in the investigated solutions of 0.4 M C_{10}TAB at 25°C, compared to results from calculations from the dressed micelle model. The ensemble average values come from accumulation over approximately 3000 configurations, taken in steps of 5 configurations over the 15000 configurations generated. The uncertainties on the values in Table 1 derived from these configurations are ± one standard deviation of the distribution of average values.

Solution	water	0.2 M HBr	0.2 M HCl
Average Number of $C_{10}TA^+$ in largest micelle	82.0±18.4	22.7±4.6	23.3±4.6
Radius of gyration of largest micelle[†] **R_g (Å)**	22.1±3.8	13.5±1.0	14.4±1.7
Spherical Compactness of largest micelle[‡]	0.14 ±0.05	0.22 ±0.10	0.17 ±0.10
Average Number of cations at surface, $N_{cations}$	48.4±6.2	20.5±3.8	19.7±3.0
Average Number of anions at surface, N_{anions}	31.6±4.7	17.9±3.9	11.4±2.8
Dissociation Parameter, β from EPSR[*]	0.35±0.06	0.12±0.13	0.41±0.13
Average Number of Br^- at micelle surface	31.6±4.7	17.9±3.9	8.4±2.2
Average Hydration Number of all Br^- **(Integrating 1.5 Å $\leq g_{Br\text{-}HW}(r) \leq$ 3.1 Å)**	4.6±0.1	4.5±0.1	5.6±0.1
Average Number of Cl^- at micelle surface	-	-	3.0±1.3
Average Hydration Number of all Cl^- **(Integrating 1.5 Å $\leq g_{Cl\text{-}HW}(r) \leq$ 2.8 Å)**	-	-	4.2±0.1
Dressed micelle model prediction[57] (β)	0.39	0.38	0.36

† R_g is the root mean square value for the distribution of surfactant atoms about the micelle centre.
‡ The spherical compactness is the ratio between the number of surfactant monomers in the micelles compared with the ideal number that could fit in a solid sphere of radius $R = R_g / \sqrt{\frac{3}{5}}$ at the atomic density of the solution. The closer the spherical compactness is to a value of 1.0, the more spherical the micelle.
* β is calculated from $1.0 - (N_{anions}/N_{cations})$ at the surface of the micelle.

In our case, in the pure water system, the average hydration number obtained by integrating $g_{Br-HW}(r)$ to 3.1Å gives a value of just under 5 water neighbours around the Br⁻ counterion. This is lower than the hydration number obtained in a simple RbBr salt solution[58] (a fully dissociated salt in aqueous solution where Br⁻ has 6 water neighbours) and is suggestive of the bromide ion being closely associated with the cationic surfactant headgroup, preventing full hydration by water. Interestingly the average hydration number for Br⁻ in the HBr system is similar to that found in the acid free system, but in the solution with added HCl, the average hydration number rises to 5.6±0.1 which is much closer to the value found in simple salt solutions. In contrast, in the HCl system, the average hydration number of Cl⁻ is lower than the expected value of 6,[59] which at 4.2±0.1 is in line with the value found for Br⁻ in the acid free and HBr solutions where the hydration shell has been perturbed by the micelle surface. Overall therefore, this is consistent with a picture for the mixed anion system in which the association of a proportion of the Cl⁻ ions with the micelle surface frees up some of the Br⁻ ions for release into the bulk aqueous environment where they can adopt their nominally preferred hydration levels.

The organisation of water and ions around the surfactant headgroups are shown by spatial density function plots, which plot the isosurface for the most likely positions of ions and water around the surfactant headgroup by taking the highest 5 or 15% probability locations for those species. For the counterions, the different ion sizes imposed by the reference potentials, and the Coulomb interactions between the charged atomic sites allow the Br⁻ and Cl⁻ to find favoured locations around the headgroup in the EPSR model, (Figure 8), showing evidence of both an inner and outer shell of organised anions. For the pure water case (Figure 8a), an inner shell of Br⁻ is, perhaps unsurprisingly, located in the regions between the methyl groups on the quaternary ammonium headgroup, with the outer shell weakly evident above the methyls, between the inner shell Br⁻ distributions. When 0.2 M HBr is added (Figure 8b) the outer shell becomes less evident at this isosurface level, and the inner shell distribution dominates the preferred ion locations around the surfactant headgroup. This gives graphical evidence of

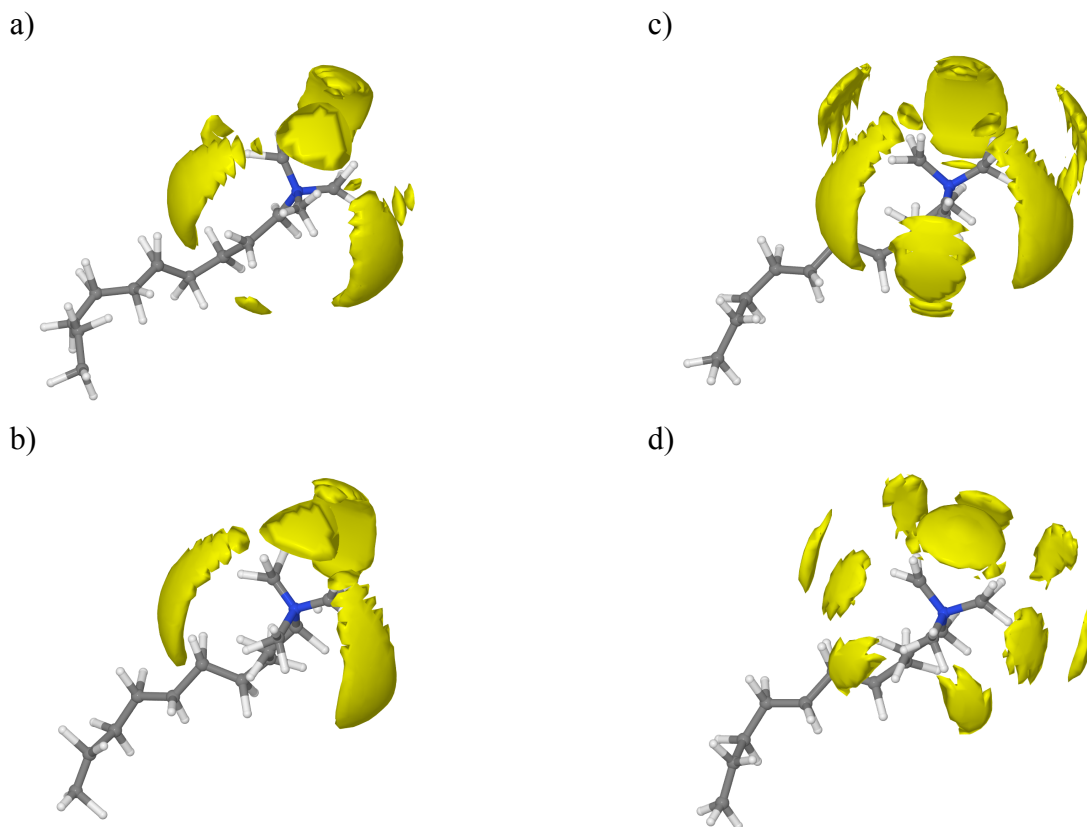the extra screening of the headgroup charge caused by addition of the strongly bound Br⁻.

a)

c)

b)

d)

Figure 8 Most likely (top 15%) isosurface for ions around C_{10}TAB molecules in micelles in a) water, Br⁻ around C_{10}TA⁺, b) 0.2 M HBr, Br⁻ around C_{10}TA⁺ c) 0.2 M HCl, Br⁻ around C_{10}TA⁺ d) 0.2 M HCl, Cl⁻ around C_{10}TA⁺. Highlights anion location around nitrogen in head group in the radial distance range from 2 to 7 Å.

In the case where 0.2 M HCl was added (figure 8c,d) it appears that while both Br⁻ and Cl⁻ are located in the first shell of anions around the quaternary ammonium headgroup, the Br⁻ locations are largely unperturbed from that observed for the pure water case, but the Cl⁻ ions occupy a range of tightly localized smaller locations within the same region occupied by the Br⁻. Additionally the Cl⁻ also occupies well-defined regions in the outer shell, but in this case Br⁻ does not appear in the second shell region, leaving this area preferentially occupied solely by Cl⁻. Note that as this representation is proportional, it does not indicate absolute numbers of counterions bound to the headgroups, only their most likely locations.
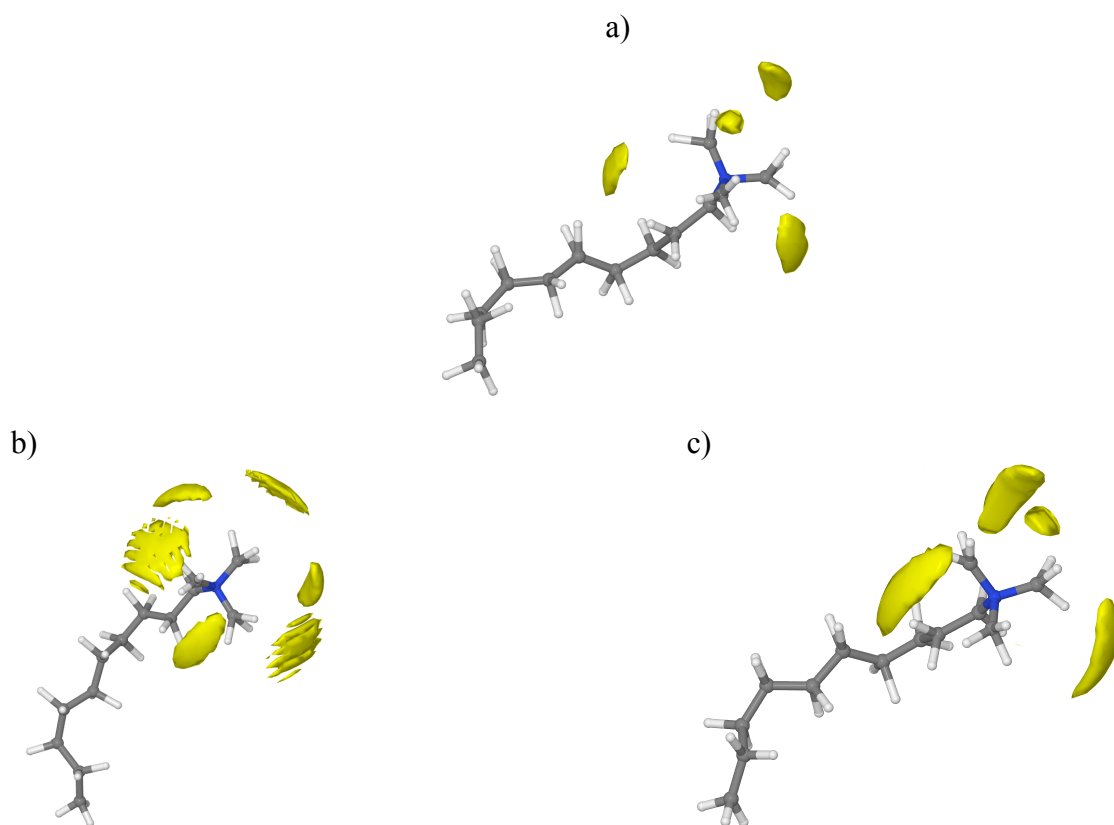
a)

b)

c)

Figure 9 Water distribution around headgroups shown by the most likely (top 5%) isosurfaces for water molecules around $C_{10}TAB$ molecules in micelles in a) water, 1st shell water 2 to 5 Å b) 0.2 M HBr, 1st shell water 2 to 5 Å c) 0.2 M HCl, 1st shell water 2 to 5 Å.

The corresponding plots for the water locations around the headgroups are shown in Figure 9, and highlight differences between the pure water, HCl and HBr cases. In pure water the presence of the counterions result in the generation of a few spatially preferred regions of water molecules around the headgroup of the surfactant that mirror the preferred Br^- locations. However for both HCl and HBr solutions, a first shell of water appears to favour an enhanced range of spatially defined positions, closer to the headgroup in several places, which, in the HBr solution are more spatially dispersed compared to those found in the pure water case, but which in the HCl solution are similar, although slightly more spread out.

The β values for the pure water case and the 0.2 M HBr solution calculated from the EPSR models indicate that 0.35 and 0.12 of the Br- counterions are dissociated respectively, although in each case the

error bars on these numbers are large (±0.13). The markedly lower degree of counterion dissociation in the presence of the HBr suggests that additional Br- ions are located in close proximity to the nitrogen containing headgroups in this system, having lost solvating water, to coordinate to the surfactant headgroups. Our result contrasts with earlier measurements of the degree of counterion dissociation for $C_{10}TAB$ in solutions with added NaBr using ultrasonic relaxation spectroscopy, where dissociation of the bromide counterions was found to be independent of salt concentrations up to 0.2 M.[37] It also contrasts with the predictions of the dressed micelle model,[57] calculated for the systems studied here, and presented in Table 1. The dressed micelle model takes account of the ionic strength in the solution from the presence of the acid, but not the specific identity of the ions used.

In comparison, the EPSR model suggests that 0.41 of the total anions are dissociated from the micelle surface in the 0.2 M HCl solution, a value much closer to, but larger than, the ion dissociation found for these micelles in pure water (β 0.35). Thus when Cl⁻ is added, despite the equivalent ionic strengths in both acid solutions, the competition for water in the anion hydration shells leads to lower ion binding at the micelle surface, reducing charge screening at the headgroup and allowing the structuring of water to extend further into solution.

Hofmeister ions are often characterised as cosmotropes or chaotropes depending on their water-structuring properties, and these interact with micelles in two ways.[24] Cosmotropes are small, highly hydrated ions and when added to a micellar solution are supposed to dehydrate the micelle surface due to competition for water by their strongly bound hydration shells. The ions themselves remain in the solution between micelles and decrease the Debye length of the solution. Chaotropes on the other hand, have more weakly bound hydration shells enabling strong adsorption of the anion to the surfactant headgroup or micelle surface despite loss of water from the anion hydration shell.[29] This enables tighter packing of the surfactant molecules due to the screening of their Coulombic repulsion.[22] The quaternary ammonium headgroup of the $C_{10}TA$ cation is classed as a chaotropic headgroup,[60-61] which

is expected to bind more strongly to chaotropic anions. Cl^- is usually classed as a weak cosmotrope while Br^- is a chaotrope,[24] and certainly the results for the HBr solutions found here accord with the strong binding of Br^- to the micelle surface, screening charge between headgroups and decreased ion dissociation.

The results in the presence of Cl^- are more ambiguous. According to the EPSR results, Cl^- addition appears to decrease the binding of all anions close to the micelle surface, although the anions are structured into two shells around the surfactant headgroups. The errors on the β values from EPSR however are rather large, so may be similar to the extent of ion binding found in the pure water solution. This would suggest that addition of Cl^- does not alter the overall number of anions bound to the micelles.

Charge screening on the headgroups is also responsible for the observed changes in micelle structure, leading to the more compact, closely packed micelles in the highly screened 0.2 M HBr case, and the looser more disordered micelle interface in the 0.2 M HCl solutions. Micelles in both solutions are however smaller and more spherically compact than those in pure water, presumably due to the overall increased ionic strength of the solution. Lee et al[62] carried out a reflectivity on the adsorbed layer of $C_{10}TAB$ at the water surface above the CMC (0.05 M) and found a staggered structure of the headgroup layer resulting from electrostatic repulsion between the head groups when these are tightly packed at the solution surface. This resulted in a headgroup layer thickness around 6-7 Å for an area per molecule around 58 $Å^2$, although they suggest that SANS measurements on $C_{10}TAB$ in pure water gave a "smooth" micelle surface with a 2-3 Å headgroup thickness for slightly larger areas per molecule ie 65 $Å^2$. In our case, the smaller micelle formed in the presence of HCl would, if the molecules remained as tightly packed as in pure water, also decrease the area per molecule at the surface of the micelle, leading to the observed disordering. However with added 0.2 M HBr, the enhanced counterion binding, resulting in further charge screening has the opposite effect, promoting a

smoother micelle interface despite the smaller micelle size in these solutions, compared to the pure water solution.

Conclusion

Wide angle neutron scattering measurements have been used to probe the extent and competition between ions bound at the surface of decyltrimethylammonium bromide micelles in acidic solutions of HCl or HBr. These experiments, combined with EPSR modelling show distinct differences between counterion binding and the micelle structures in these solutions. In 0.2 M HBr solution the micelles are more compact, dehydrated and spherical, with tightly bound bromide anions present at the surface of the micelles. In 0.2 M HCl solution by comparision the micelles are less well ordered, and the extent of anion binding to the micelle surface is much lower. In both cases the micelles are smaller than in pure water, having aggregation numbers 4 times lower than in water, and radii around 14 Å, compared to 22 Å in water. The differences between the HBr and HCl systems are attributed to differences in the anion hydration and extent of binding to the surfactant headgroups, and these follow the predictions of the Hofmeister series.

Supporting Information Available

Table of Lennard-Jones and Coulomb parameters used for the reference potentials. EPSR model fits to the diffraction data for 0.4 M C_{10}TAB in 0.2 M HBr or in water. Unnormalized pair distribution functions calculated from these EPSR models for the 0.4 M C_{10}TAB with 0.2 M HCl, or with 0.2 M HBr data, at 25 °C.

Acknowledgments

24

References

(1) Evans, D. F.; Wennerström, H., *The Colloidal Domain: Where Physics, Chemistry, Biology, and Technology Meet*. 2nd ed.; Wiley-VCH: New York, 1999.

(2) Yang, H.; Coombs, N.; Ozin, G. A., Morphogenesis of Shapes and Surface Patterns in Mesoporous Silica. *Nature* **1997,** *386*, 692-695.

(3) Ozin, G. A.; Yang, H.; Sokolov, I.; Coombs, N., Shell Mimetics. *Adv. Mater.* **1997,** *9*, 662-667.

(4) Chan, H. B. S.; Budd, P. M.; Naylor, T. deV., Control of Mesostructured Silica Particle Morphology. *J. Mater. Chem.* **2001,** *11*, 951-957.

(5) Brennan, T.; Hughes, A. V.; Roser, S. J.; Mann, S.; Edler, K. J., Concentration-Dependent Formation Mechanisms in Mesophase Silica-Surfactant Films. *Langmuir* **2002,** *18*, 9838-9844.

(6) Brinker, C. J.; Scherer, G. W., *Sol-Gel Science. The Physics and Chemistry of Sol-Gel Processing*. Academic Press: San Diego, 1990.

(7) Huo, Q.; Margolese, D. I.; Ciesa, U.; Feng, P.; Gier, T. E.; Sieger, P.; Leon, R.; Petroff, P. M.; Schüth, F.; Stucky, G. D., Generalised Synthesis of Periodic Surfactant/Inorganic Composite Materials. *Nature* **1994,** *368*, 317-321.

(8) Che, S.; Li, H.; Lim, S.; Sakamoto, Y.; Terasaki, O.; Tatsumi, T., Synthesis Mechanism of Cationic Surfactant Templating Mesoporous Silica under an Acidic Synthesis Process. *Chem. Mater.* **2005,** *17*, 4103-4113.

(9) Edler, K. J.; White, J. W., Further Improvements in the Long Range Order of Mcm-41 Materials. *Chem. Mater.* **1997,** *9*, 1226-1233.

(10) Lin, H. P.; Kao, C. P.; Mou, C. Y., Counterion and Alcohol Effect in the Formation of Mesoporous Silica. *Microporous Mesoporous Mater.* **2001,** *48*, 135-141.

(11) Bunton, C. A., Chemical Reactivity in Micelles and Similar Assemblies of Cationic Surfactants. In *Cationic Surfactants: Physical Chemistry*, Rubingh, D. N.; Holland, P. M., Eds. Marcel Dekker: New

York & Basel, 1991; Vol. 37, pp 323-405.

(12) Lebedeva, N.; Zana, R.; Bales, B. L., A Reinterpretation of the Hydration of Micelles of Dodecyltrimethylammonium Bromide and Chloride in Aqueous Solution. *J. Phys. Chem. B* **2006**.

(13) Zana, R., Ionization of Cationic Micelles: Effect of the Detergent Structure. *J. Colloid Interface Sci.* **1980,** *78*, 330-337.

(14) Loughlin, J. A.; Romsted, L. S., A New Method for Estimating Counterion Selectivity of a Cationic Association Colloid - Trapping of Interfacial Chloride and Bromide Counterions by Reaction Wtih Micellar Bound Aryldiazonium Salts. *Colloids and Surfaces* **1990,** *48*, 123-137.

(15) Cuccovia, I. M.; da Silva, I. N.; Chaimovich, H.; Romsted, L. S., New Method for Estimating the Degree of Ionization and Counterion Selectivity of Cetyltrimethylammonium Halide Micelles: Chemical Trapping of Free Counterions by a Water Soluble Arenediazonium Ion. *Langmuir* **1997,** *13*, 647-652.

(16) Abuin, E.; Lissi, E., Competitive Binding of Counterions at the Surface of Mixed Ionic/Nonionic Micelles: Application of the Ion Exchange Formalism. *J. Colloid Interface Sci.* **1991,** *143*, 97-102.

(17) Long, J. A.; Rankin, B. M.; Ben-Amotz, D., Micelle Structure and Hydrophobic Hydration. *J. Am. Chem. Soc.* **2015,** *137*, 10809-10815.

(18) van der Post, S. T.; Hunger, J.; Bonn, M.; Bakker, H. J., Observation of Water Separated Ion-Pairs between Cations and Phospholipid Headgroups. *J. Phys. Chem. B* **2014,** *118*, 4397-4403.

(19) Pokorna, S.; Jurkiewicz, P.; Cwiklik, L.; Vazdar, M.; Hof, M., Interactions of Monovalent Salts with Cationic Lipid Bilayers. *Faraday Discuss.* **2013,** *160*, 341-358.

(20) Murdachaew, G.; Valiev, M.; Kathmann, S. M.; Wang, X.-B., Study of Ion Specific Interactions of Alkali Cations with Dicarboxylate Dianions. *J. Phys. Chem. A* **2012,** *116*, 2055-2061.

(21) Lindman, B.; Puyal, M. C.; Kamenka, N.; Brun, B.; Gunnarsson, G., Micelle Formation of Ionic Surfactants. Tracer Self-Diffusion Studies and Theoretical Calculations for Sodium P-Octylbenzenesulfonate. *J. Phys. Chem.* **1982,** *86*, 1702-1711.

(22) Oelschlaeger, C.; Suwita, P.; Willenbacher, N., Effect of Counterion Binding Efficiency on Structure and Dynamics of Wormlike Micelles. *Langmuir* **2010,** *26*, 7045-7053.

(23) Ivanov, I. B.; Slavchov, R. I.; Basheva, E. S.; Sidzhakova, D.; Karakashev, S. I., Hofmeister Effect on Micellization, Thin Films and Emulsion Stability. *Adv. Colloid Interface Sci.* **2011,** *168*, 93-104.

(24) Akpinara, E.; Reis, D.; Martins Figueiredo Neto, A., Effect of Hofmeister Anions on the Existence of the Biaxial Nematic Phase in Lyotropic Mixtures of Dodecyltrimethylammonium Bromide/Sodium Salt/1-Dodecanol/Water. *Liq. Cryst.* **2015,** *42*, 973-981.

(25) Berkowitz, M. L.; Vácha, R., Aqueous Solutions at the Interface with Phospholipid Bilayers. *Acc. Chem. Res.* **2012,** *45*, 74–82.

(26) Fox, J. M.; Kang, K.; Sherman, W.; Héroux, A.; Sastry, G. M.; Baghbanzadeh, M.; Lockett, M. R.; Whitesides, G. M., Interactions between Hofmeister Anions and the Binding Pocket of a Protein. *J. Am. Chem. Soc.* **2015,** *137*, 3859-3866.

(27) Jungwirth, P.; Cremer, P. S., Beyond Hofmeister. *Nat Chem* **2014,** *6*, 261-263.

(28) Parsons, D. F.; Bostrom, M.; Nostro, P. L.; Ninham, B. W., Hofmeister Effects: Interplay of Hydration, Nonelectrostatic Potentials, and Ion Size. *Phys. Chem., Chem. Phys.* **2011,** *13*, 12352-12367.

(29) Salis, A.; Ninham, B. W., Models and Mechanisms of Hofmeister Effects in Electrolyte Solutions, and Colloid and Protein Systems Revisited. *Chem. Soc. Rev.* **2014,** *43*, 7358-7377.

(30) Zhang, Y.; Cremer, P. S., Chemistry of Hofmeister Anions and Osmolytes. *Annu. Rev. Phys. Chem.* **2010,** *61*, 63-83.

(31) Xie, W. J.; Gao, Y. Q., A Simple Theory for the Hofmeister Series. *J. Phys. Chem. Lett.* **2013,** *4*, 4247-4252.

(32) Sung, W.; Wang, W.; Lee, J.; Vaknin, D.; Kim, D., Specificity and Variation of Length Scale over Which Monovalent Halide Ions Neutralize a Charged Interface. *J. Phys. Chem. C* **2015,** *119*, 7130-7137.

(33) Wang, W.; Sung, W.; Ao, M.; Anderson, N. A.; Vaknin, D.; Kim, D., Halide Ions Effects on Surface Excess of Long Chain Ionic Liquids Water Solutions. *J. Phys. Chem. B* **2013,** *117*, 13884-13892.

(34) Ninham, B. W.; Duignan, T. T.; Parsons, D. F., Approaches to Hydration, Old and New: Insights through Hofmeister Effects. *Curr. Op. Colloid Interface Sci.* **2011,** *16*, 612-617.

(35) Brennan, T.; Roser, S. J.; Mann, S.; Edler, K. J., Characterisation of the Structure of Mesoporous Thin Films Grown at the Air/Water Interface Using X-Ray Surface Techniques. *Langmuir* **2003,** *19*, 2639-2642.

(36) Debye, P., Light Scattering in Soap Solutions. *Ann. N.Y. Acad. Sci.* **1949,** *51*, 575-592.

(37) Nomura, H.; Koda, S.; Matsuoka, T.; Hiyama, T.; Shibata, R.; Kato, S., Study of Salt Effects on the Micelle–Monomer Exchange Process of Octyl-, Decyl-, and Dodecyltrimethylammonium Bromide in Aqueous Solutions by Means of Ultrasonic Relaxation Spectroscopy. *J. Colloid Interface Sci.* **2000,** *230*, 22-28.

(38) Yoshida, N.; Matsuoka, K.; Moroi, Y., Micelle Formation of N-Decyltrimethylammonium Perfluorocarboxylates. *J. Colloid Interface Sci.* **1997,** *187*, 388-395.

(39) Holmberg, K.; Jönsson, B.; Kronberg, B.; Lindman, B., *Surfactants and Polymers in Aqueous Solution*. John Wiley & Sons Ltd: Chichester, England, 2002.

(40) Keiper, J.; Romsted, L. S.; Yao, J.; Soldi, V., Interfacial Compositions of Cationic and Mixed Non-Ionic Micelles by Chemical Trapping: A New Method for Characterizing the Properties of Amphiphilic Aggregates. *Colloids Surf. A* **2001,** *176*, 53-67.

(41) Aswal, V. K.; Goyal, P. S., Dependence of the Size of Micelles on the Salt Effect in Ionic Micellar Solutions. *Chem. Phys. Lett.* **2002,** *364*, 44-50.

(42) Aswal, V. K.; Goyal, P. S., Role of Different Counterions and Size of Micelle in Concentration Dependence Micellar Structure of Ionic Surfactants. *Chem. Phys. Lett.* **2003,** *368*, 59-65.

(43) Romsted, L. S., Do Amphiphile Aggregate Morphologies and Interfacial Compositions Depend

Primarily on Interfacial Hydration and Ion-Specific Interactions? The Evidence from Chemical Trapping. *Langmuir* **2007,** *23*, 414-424.

(44) Zajforoushan Moghaddam, S.; Thormann, E., Hofmeister Effect of Salt Mixtures on Thermo-Responsive Poly(Propylene Oxide). *Phys. Chem., Chem. Phys.* **2015,** *17*, 6359-6366.

(45) Hargreaves, R.; Bowron, D. T.; Edler, K. J., The Atomistic Structure of a Micelle in Solution Determined by Wide Q-Range Neutron Diffraction. *J. Am. Chem. Soc.* **2011,** *133*, 16524-16536.

(46) Soper, A. K., Partial Structure Factors from Disordered Materials Diffraction Data: An Approach Using Empirical Potential Structure Refinement. *Phys. Rev. B* **2005,** *72*, 104204.

(47) Mukherjee, P.; Mysels, K. J., Critical Micelle Concentrations of Aqueous Surfactant Systems. *Nat. Stand. Ref. Data Ser. Nat. Bur. Stand.* **1971**.

(48) Buckingham, S. A.; Garvey, C. J.; Warr, G. G., Effect of Head-Group Size on Micellization and Phase Behavior in Quaternary Ammonium Surfactant Systems. *J. Phys. Chem.* **1993,** *97*, 10236-10244.

(49) Chakraborty, I.; Moulik, S. P., Self-Aggregation of Ionic C10 Surfactants Having Different Headgroups with Special Reference to the Behavior of Decyltrimethylammonium Bromide in Different Salt Environments: A Calorimetric Study with Energetic Analysis. *J. Phys. Chem. B* **2007,** *111*, 3658-3664.

(50) D'Errico, G.; Ortona, O.; Paduano, L.; Vitagliano, V., Transport Properties of Aqueous Solutions of Alkyltrimethylammonium Bromide Surfactants at 25°C. *J. Colloid Interface Sci.* **2001,** *239*, 264-271.

(51) Eckold, G.; Gorski, N., Small-Angle Neutron Scattering from Tetradecyltrimethylammonium Bromide in Nabr Aqueous Solutions. *Colloids Surf. A* **2001,** *183*, 361-369.

(52) Slavchov, R. I.; Karakashev, S. I.; Ivanov, I. B., Ionic Surfactants and Ion-Specific Effects: Adsorption, Micellization, Thin Liquid Films. In *Surfactant Science and Technology: Retrospects and Prospects* Romsted, L. S., Ed. Taylor & Francis Group: 2014; p 528.

(53) Morgan, J. D.; Napper, D. H.; Warr, G. G., Thermodynamics of Ion Exchange Selectivity at

Interfaces. *J. Phys. Chem.* **1995,** *99*, 9458-9465.

(54) Abuin, E. B.; Lissi, E.; Araujo, P. S.; Aleixo, R. M. V.; Chaimovich, H.; Bianchi, N.; Miola, L.; Quina, F. H., Selectivity Coefficients for Ion Exchange in Micelles of Hexadecyltrimethylammonium Bromide and Chloride. *J. Colloid Interface Sci.* **1983,** *96*, 293-295.

(55) Soldi, V.; Keiper, J.; Romsted, L. S.; Cuccovia, I. M.; Chaimovich, H., Arenediazonium Salts: New Probes of the Interfacial Compositions of Association Colloids. 6. Relationships between Interfacial Counterion and Water Concentrations and Surfactant Headgroup Size, Sphere-to-Rod Transitions, and Chemical Reactivity in Cationic Micelles†. *Langmuir* **2000,** *16*, 59-71.

(56) Scarpa, M. V.; Maximiano, F. A.; Chaimovich, H.; Cuccovia, I. M., Interfacial Concentrations of Chloride and Bromide and Selectivity for Ion Exchange in Vesicles Prepared with Dioctadecyldimethylammonium Halides, Lipids, and Their Mixtures. *Langmuir* **2002,** *18*, 8817-8823.

(57) Hayter, J. B., A Self-Consistent Theory of Dressed Micelles. *Langmuir* **1992,** *8*, 2873-2876.

(58) Bowron, D. T., Comprehensive Structural Modelling of Aqueous Solutions Using Neutron Diffraction and X-Ray Absorption Spectroscopy. *J. Phys. Conf. Ser.* **2009,** *190*, 012022.

(59) Soper, A. K.; Weckström, K., Ion Solvation and Water Structure in Potassium Halide Aqueous Solutions. *Biophys. Chem.* **2006,** *124*, 180-191.

(60) Marcus, Y., Effect of Ions on the Structure of Water: Structure Making and Breaking. *Chem. Rev.* **2009,** *109*, 1346-1370.

(61) Vlachy, N.; Jagoda-Cwiklik, B.; Vácha, R.; Touraud, D.; Jungwirth, P.; Kunz, W., Hofmeister Series and Specific Interactions of Charged Headgroups with Aqueous Ions. *Adv. Colloid Interface Sci.* **2009,** *146*, 42-47.

(62) Lee, E. M.; Thomas, R. K.; Penfold, J.; Ward, R. C., Structure of Aqueous Decyltrimethylammonium Bromide Solutions at the Air Water Interface Studied by the Specular Reflection of Neutrons. *J. Phys. Chem.* **1989,** *93*, 381-388.

Table of Contents Graphic